

1 **Piezo1-mediated mechanotransduction enhances macrophage**
2 **oxLDL uptake and atherogenesis**

3
4 Hamza Atcha^{1,2}, Daanish Kulkarni^{3,4}, Vijaykumar S. Meli^{3,4,5}, Praveen Krishna
5 Veerasubramanian^{3,4}, Yuchun Wang^{3,4}, Michael D. Cahalan⁶, Medha M. Pathak^{3,6,7}, and
6 Wendy F. Liu^{3,4,5,8}

7
8 ¹ Department of Bioengineering, University of California, San Diego, La Jolla, USA
9 ² Sanford Consortium for Regenerative Medicine, La Jolla, USA
10 ³ Department of Biomedical Engineering, University of California, Irvine, Irvine, USA
11 ⁴ The Edwards Lifesciences Center for Advanced Cardiovascular Technology, University of California,
12 Irvine, Irvine, USA
13 ⁵ Department of Chemical and Biomolecular Engineering, University of California, Irvine, Irvine, USA
14 ⁶ Department of Physiology and Biophysics, University of California Irvine, Irvine, USA
15 ⁷ Sue and Bill Gross Stem Cell Research Center, University of California, Irvine, Irvine, USA
16 ⁸ Department of Molecular Biology and Biochemistry, University of California, Irvine, Irvine, USA

17
18
19 Correspondence should be addressed to W.F.L. (email: wendy.liu@uci.edu)
20

1 **Abstract**

2 Macrophages in the vascular wall ingest and clear lipids, but abundant lipid accumulation leads to foam
3 cell formation and atherosclerosis, a pathological condition often characterized by tissue stiffening. While
4 the role of biochemical stimuli in the modulation of macrophage function is well studied, the role of
5 biophysical cues and the molecules involved in mechanosensation are less well understood. Here, we use
6 genetic and pharmacological tools to show extracellular oxidized low-density lipoproteins stimulate Ca^{2+}
7 signaling through activation of the mechanically gated ion channel Piezo1. Moreover, macrophage Piezo1
8 expression is critical in the transduction of environmental stiffness and channel deletion suppresses,
9 whereas a gain-of-function mutation exacerbates oxLDL uptake. Additionally, we find that depletion of
10 myeloid Piezo1 protects from atherosclerotic plaque formation *in vivo*. Together, our study highlights an
11 important role for Piezo1 and its respective mutations in macrophage mechanosensing, lipid uptake, and
12 cardiovascular disease.

14 **Keywords:** macrophage, mechanotransduction, Piezo1, atherosclerosis, foam cell, cardiovascular disease

16 **Significance Statement**

17 The mechanically gated ion channel Piezo1 has recently been shown to play a major role in macrophage
18 mechanotransduction and is involved in numerous pathologies. However, its role in atherosclerosis and
19 cardiovascular disease is poorly understood. Here, we show that Piezo1 enhances macrophage uptake of
20 oxLDL, a major lipid component of foam cells within atherosclerotic plaques. Additionally, we show that
21 mutations in this channel can modulate progression of atherosclerosis. Channel depletion reduces oxLDL
22 uptake and protects from disease, whereas a gain of function point mutation, which is common among
23 individuals of African descent, enhances oxLDL uptake. Our study reveals a critical role for Piezo1 in
24 atherosclerosis and highlights a potential new therapeutic target for treatment of disease.

25

1 **Introduction**

2 Macrophages are mechanosensitive cells of the innate immune system that are central regulators of
3 atherosclerosis and cardiovascular disease. These innate immune cells are recruited to the arterial wall,
4 where they are responsible for the ingestion and removal of circulating lipids such as oxidized low-density
5 lipoproteins (oxLDLs) (1). Uptake of oxLDL in macrophages is largely controlled by scavenger receptors
6 including CD36 and SRA1 (2), which recognize and bind oxLDL uptake as well as apoptotic cells,
7 glycated proteins, and amyloid forming peptides (3, 4). Moreover, the expression of these receptors is
8 regulated by exposure to lipids as well as their transport and metabolism within cells. Elevated plasma
9 cholesterol and inefficient systemic clearance results in enhanced cholesterol uptake and the formation of
10 foam cells that are rich in lipid droplets. Continued and excessive cholesterol loading triggers apoptosis
11 of foam cells initiating the development of a necrotic core in an atherosclerotic plaque. Plaque formation
12 also results in deposition of abundant extracellular matrix proteins, including fibronectin, and is associated
13 with stiffening of the arterial microenvironment (5–7). While it is well-appreciated that disease alters
14 tissue mechanics, the role of mechanical cues and mechanosensitive molecules in regulating macrophage
15 function and lipid uptake in atherosclerosis remains understudied.

16 The mechanosensitive ion channel Piezo1 has recently been shown to play a major role in
17 macrophage function (8) and mutations to this channel are implicated in several diseases (9). Piezo1
18 specific mutations have been shown to lead to lymphatic dysplasia (10), which is caused by Piezo1 loss-
19 of-function (LOF) (11, 12). Gain-of-function (GOF) point mutations, on the other hand, slow channel
20 inactivation and therefore enhance ion movement through the channel (13). In mice, the R2482H Piezo1
21 GOF mutations (equivalent to R2456H in humans and affecting 30% of individuals in African
22 populations) increased macrophage phagocytotic activity, resulting in compromised iron metabolism and
23 heightened red blood cell turnover (9). Additionally, the GOF mutation was found to reduce parasitemia
24 in human red blood cells in vitro and protect mice from cerebral malaria (14). However, while

1 cardiovascular diseases are also known to be more prevalent within the same racial and ethnic group (15),
2 the role of these mutations in atherosclerosis and cardiovascular disease is unknown.

3 In this study, we examine the role of Piezo1 in the modulation of macrophage oxLDL uptake and
4 atherosclerotic plaque formation. We utilize genetic mouse models with Piezo1 depletion (*Piezo1^{ΔLysM}*) or
5 GOF mutations (*Piezo1^{LysM-GOF}*) in myeloid cells and found that oxLDL stimulated Ca²⁺ influx in a Piezo1-
6 dependent manner and that Piezo1 activity enhanced oxLDL uptake *in vitro* and promoted atherosclerotic
7 plaque formation *in vivo*. Our study identifies Piezo1 as a critical mechanosensitive molecule involved in
8 foam cell formation as well as atherosclerotic plaque development and progression.

10 Results

11 Piezo1 depletion reduces Ca²⁺ influx and oxLDL uptake

12 Using siRNA or transgenic mice with channel depletion (16, 17), we first examined the role of
13 Piezo1 in modulating Ca²⁺ events, uptake, stiffness mechanotransduction, and responses to oxLDL. We
14 observed that oxLDL treatment enhanced Ca²⁺ events and that siRNA mediated Piezo1 knockdown
15 abrogated this increased activity (**Fig. 1a-c**). Functionally, we found that oxLDL accumulation was
16 reduced in cells lacking Piezo1 (*Piezo1^{ΔLysM}*) and consistent with this observation, cells had reduced CD36
17 and SRA1 uptake receptor expression when treated with oxLDL (**Fig. 1d-e**). In contrast, control Piezo1-
18 expressing cells increased uptake and expression of receptors in response to oxLDL treatment (**Fig. 1e**).
19 However, no differences in oxLDL binding to the cell surface were observed between control and Piezo1
20 lacking macrophages suggesting that Piezo1 primarily modulates oxLDL internalization. Moreover, given
21 that Piezo1 is a mechanically gated ion channel, which has been shown to sense and transduce a variety
22 of different physical cues, and that atherosclerosis is often associated with stiffening of the arterial
23 microenvironment, we next evaluated the role of substrate stiffness in regulating Piezo1 mediated oxLDL
24 uptake. Atherosclerotic plaque development has been shown to result in localized areas of enhanced
25 stiffness within the artery, with regions measuring ~250 kPa using atomic force microscopy (18).

1 Therefore, we cultured macrophages on fibronectin- conjugated polyacrylamide hydrogels representing a
2 soft (1 kPa) or stiff (280 kPa) microenvironment and stimulated cells with oxLDL. We found that stiffness
3 enhanced oxLDL uptake in control macrophages, and that *Piezo1^{ΔLysM}* reduced oxLDL uptake on stiff
4 substrates when compared to control (**Fig. 1f**). Additionally, significant differences in oxLDL uptake were
5 also observed between Piezo1 deficient cells cultured on 1 kPa and 280 kPa surfaces. Given that ion
6 channel depletion did not fully abrogate increased oxLDL uptake on stiff surfaces, it is plausible that
7 Piezo1 independent mechanisms are also involved (**Fig. 1f**). Together, our data suggests that Piezo1 is
8 activated in response to oxLDL treatment, and its depletion reduces oxLDL uptake on stiff surfaces.

10 **Piezo1 GOF promotes uptake through modulation of oxLDL receptor expression**

11 In contrast to Piezo1 depletion, Piezo1 GOF (*Piezo1^{LysM-GOF}*) exhibited enhanced oxLDL uptake
12 compared to control cells and showed increased SRA1 uptake receptor expression, both with and without
13 oxLDL stimulation (**Fig. 2a-b**). *Piezo1^{LysM-GOF}* also exhibited enhanced oxLDL uptake on soft surfaces
14 when compared to control cells (**Fig. 2c**). Together, our data suggests an important role for Piezo1 in the
15 modulation of oxLDL uptake, with Piezo1 GOF positively associated with uptake receptor expression and
16 resulting in oxLDL accumulation within cells. When combined, our data suggests that Piezo1 GOF
17 mutation enhances oxLDL uptake through increases in uptake receptor expression and can promote
18 mechanotransduction on soft surfaces.

20 **Piezo1 is highly expressed within and enhances atherosclerotic plaque development**

21 Finally, we evaluated the role of Piezo1 in modulating atherosclerosis *in vivo* using a mouse model.
22 We used liver targeted adenoviral overexpression of murine PCSK9, which increases the degradation of
23 LDLR, and also regulates triglycerides in the small intestine and modulates megalin-driven protein
24 reabsorption in the kidney (19–21). When combined with a high fat diet, PCSK9 elevates systemic
25 cholesterol levels in mice resulting in atherosclerotic plaque formation (20, 22). Following three months

1 on a high fat diet we observed enhanced *Piezo1* gene expression localized to atherosclerotic plaques within
2 AAV-PCSK9 treated mice when compared to control, suggesting a potential role for Piezo1 in plaque
3 development and progression *in vivo* (**Fig. 3a**). We treated control and *Piezo1^{ALysM}* mice with AAV-
4 PCSK9 and found that *Piezo1^{ALysM}* mice had reduced plaque formation when compared to control mice
5 expressing Piezo1 (**Fig. 3b-c**). Interestingly, while both en-face and histological staining indicate
6 significant reduction in plaque formation, histology sections suggest a more profound effect on plaque
7 development, as measured by reduced vessel closure in mice lacking myeloid Piezo1 (**Fig. 3c**). Together,
8 the data presented in this study provide key insights into the role of Piezo1 in the mechanosensation of
9 stiffness as well as the modulation of oxLDL uptake and atherosclerotic plaque formation.

11 Discussion

12 Our study suggests an important role for Piezo1 in oxLDL uptake and atherosclerosis. While other
13 channels, such as TRPM7 and Orai1, have been shown to regulate Ca²⁺ activity in response to oxLDL as
14 well as inflammatory stimuli in macrophages (23, 24), our data show that Piezo1 is required for Ca²⁺
15 influx in response to oxLDL stimulation. The molecular mediators responsible for atherosclerosis are still
16 being elucidated; however, shear stress and stiff environments have been shown to enhance oxLDL uptake
17 (25, 26). Recent studies have uncovered the importance of Piezo1 in regulating cell morphology and
18 mechanotransduction pathways across a variety of developmental and pathological conditions involving
19 macrophages (8, 16). We show that Piezo1 plays a pivotal role in sensing stiff environments, modulating
20 the expression of key uptake transporters, enhancing oxLDL accumulation, and leading to macrophage
21 foam cell formation *in vitro* and the development and progression of atherosclerosis *in vivo*. Interestingly,
22 while it is known that oxLDL transporter expression is tightly regulated through positive feedback
23 mechanisms involving a number of different signaling pathways such as NFkB or PPAR γ , our data suggest
24 that Piezo1 may be critical to and enhances these processes (27–29).

1 Our work also utilizes genetic tools to evaluate the role of Piezo1 mutations in oxLDL uptake and
2 atherosclerosis. Our data suggests that *Piezo1^{LysM-GOF}* enhances macrophage oxLDL uptake and receptor
3 expression. These Piezo1 GOF mutations are known to be prevalent in approximately 30% of individuals
4 of African descent (14). This also correlates with increased prevalence and risk of cardiovascular disease
5 among individuals of the same ethnicity (15, 30), although no direct link has thus far been established. It
6 is plausible that while socioeconomic, underlying disease, and lifestyle are often implicated, genetic
7 mutations to the Piezo1 channel could also contribute as a risk factor in cardiovascular disease. In contrast,
8 *Piezo1^{ΔLysM}* reduces uptake and suppresses atherosclerotic plaque formation within mice. Our study,
9 combined with recent findings highlighting the role of GOF mutations in murine cardiac hypertrophy and
10 fibrosis (31), suggest that the development of Piezo1-specific inhibitors could potentially reduce
11 atherosclerotic plaque development and may also help alleviate other cardiovascular diseases. However,
12 further studies will be needed to show whether Piezo1 and its respective mutations provide additional risk
13 for disease in humans. Moreover, stiffness measurements, characterization of receptor expression of
14 explanted aortas and in vivo cholesterol modulation, as well as detailed mechanistic studies will provide
15 more insight into Piezo1-mediated molecular pathways involved in cardiovascular disease.

17 **Materials and Methods**

18 All animal experiments were approved by the University of California, Irvine's Institutional Animal Care
19 and Use Committee (IACUC) under protocol # AUP-20-047. Extended methods provided in the
20 Supplemental Information.

22 **Data availability**

23 All data supporting the key findings of this study are available within the article and its Supplementary
24 Information files. Extended methods can be found in Supplementary Information.

1
2
3
4
5
6
7
8
9
10
11
12
13
14
15
16
17
18
19
20
21
22
23

Acknowledgements

We would like to acknowledge and thank Dr. Ardem Patapoutian and Dr. Shang Ma for their support and for providing Piezo1 GOF cells as well as Dr. Raji Nagalla for help with rheometry.

Funding

This work was supported by the NIH/NIAID Grants R21AI128519-01 and R01AI151301, NIH/NIBIB Grant R21EB027840-01, and NIH/NIAMS Grant R21AR077288 to W.F.L.; NIH/NIAID R01AI121945 and NIH/NINDS R01NS14609 to M.D.C.; and NIH Director's Fund DP2AT010376 and NIH/NINDS R01NS109810 to M.M.P. H.A. was supported by NIH/NHLBI T32 Training Grant T32HL007444. This study was made possible, in part, through access to the Optical Biology Core Facility of the Developmental Biology Center, a shared resource supported by the Cancer Center Support Grant (CA-62203) and Center for Complex Biological Systems Support Grant (GM-076516) at the University of California, Irvine and through access to a confocal microscope within the UCI Edwards Lifesciences Foundation Cardiovascular Innovation and Research Center supported by (1S10OD025064-01A1) and the microscope imaging core within the Sue and Bill Gross Stem Cell Research Center at the University of California, Irvine.

Author Contributions

H.A., D.K., V.S.M, P.V. and Y.W. performed experiments. H.A. and D.K. collected and analyzed data. H.A., M.D.C, M.M.P., and W.F.L. designed experiments and wrote the manuscript.

Competing Interests Statement

The authors declare no competing interests.

References

1. Y. V. Bobryshev, E. A. Ivanova, D. A. Chistiakov, N. G. Nikiforov, A. N. Orekhov, Macrophages and Their Role in Atherosclerosis: Pathophysiology and Transcriptome Analysis. *Biomed Res Int* **2016** (2016).
2. K. J. Moore, M. W. Freeman, Scavenger Receptors in Atherosclerosis: Beyond Lipid Uptake. *Arteriosclerosis, Thrombosis, and Vascular Biology* **26**, 1702–1711 (2006).
3. R. L. Silverstein, M. Febbraio, CD36, a scavenger receptor involved in immunity, metabolism, angiogenesis, and behavior. *Sci Signal* **2**, re3 (2009).
4. E. Linares-Alcántara, F. Mendlovic, Scavenger Receptor A1 Signaling Pathways Affecting Macrophage Functions in Innate and Adaptive Immunity. *Immunol Invest* **51**, 1725–1755 (2022).
5. A. Yurdagul, A. C. Finney, M. D. Woolard, A. W. Orr, The arterial microenvironment: the where and why of atherosclerosis. *Biochemical Journal* **473**, 1281–1295 (2016).
6. K. J. Moore, E. A. Fisher, The double-edged sword of fibronectin in atherosclerosis. *EMBO Molecular Medicine* **4**, 561–563 (2012).
7. I. Rohwedder, *et al.*, Plasma fibronectin deficiency impedes atherosclerosis progression and fibrous cap formation. *EMBO Molecular Medicine* **4**, 564–576 (2012).
8. H. Atcha, *et al.*, Ion channel mediated mechanotransduction in immune cells. *Current Opinion in Solid State and Materials Science* **25**, 100951 (2021).
9. S. Ma, *et al.*, A role of PIEZO1 in iron metabolism in mice and humans. *Cell* **184**, 969–982.e13 (2021).
10. V. Lukacs, *et al.*, Impaired PIEZO1 function in patients with a novel autosomal recessive congenital lymphatic dysplasia. *Nat Commun* **6**, 8329 (2015).
11. J. Albuissou, *et al.*, Dehydrated hereditary stomatocytosis linked to gain-of-function mutations in mechanically activated PIEZO1 ion channels. *Nat Commun* **4**, 1884 (2013).
12. R. Zarychanski, *et al.*, Mutations in the mechanotransduction protein PIEZO1 are associated with hereditary xerocytosis. *Blood* **120**, 1908–1915 (2012).
13. S. L. Alper, Genetic Diseases of PIEZO1 and PIEZO2 Dysfunction. *Curr Top Membr* **79**, 97–134 (2017).
14. S. Ma, *et al.*, Common PIEZO1 Allele in African Populations Causes RBC Dehydration and Attenuates Plasmodium Infection. *Cell* **173**, 443–455.e12 (2018).
15. Z. Javed, *et al.*, Race, Racism, and Cardiovascular Health: Applying a Social Determinants of Health Framework to Racial/Ethnic Disparities in Cardiovascular Disease. *Circulation: Cardiovascular Quality and Outcomes* **15**, e007917 (2022).
16. H. Atcha, *et al.*, Mechanically activated ion channel Piezo1 modulates macrophage polarization and stiffness sensing. *Nat Commun* **12**, 3256 (2021).
17. H. Atcha, *et al.*, Crosstalk Between CD11b and Piezo1 Mediates Macrophage Responses to Mechanical Cues. *Frontiers in Immunology* **12**, 3505 (2021).
18. P. Tracqui, *et al.*, Mapping elasticity moduli of atherosclerotic plaque in situ via atomic force microscopy. *Journal of Structural Biology* **174**, 115–123 (2011).
19. S. Rashid, *et al.*, PCSK9 Promotes Intestinal Overproduction of Triglyceride-Rich Apolipoprotein-B Lipoproteins Through Both LDL-Receptor Dependent and Independent Mechanisms. *Circulation* **130**, 431–441 (2014).
20. S. Kumar, D.-W. Kang, A. Rezvan, H. Jo, Accelerated atherosclerosis development in C57Bl6 mice by overexpressing AAV-mediated PCSK9 and partial carotid ligation. *Laboratory Investigation* **97**, 935–945 (2017).
21. C. K. Skeby, *et al.*, Proprotein convertase subtilisin/kexin type 9 targets megalin in the kidney proximal tubule and aggravates proteinuria in nephrotic syndrome. *Kidney International* **104**, 754–768 (2023).
22. C. Goettsch, *et al.*, A single injection of gain-of-function mutant PCSK9 adeno-associated virus vector induces cardiovascular calcification in mice with no genetic modification. *Atherosclerosis* **251**, 109–118 (2016).
23. B. Dutta, R. Goswami, S. O. Rahaman, TRPV4 Plays a Role in Matrix Stiffness-Induced Macrophage Polarization. *Front. Immunol.* **11** (2020).
24. M. S. Schappe, *et al.*, Chanzyme TRPM7 Mediates the Ca²⁺ Influx Essential for Lipopolysaccharide-Induced Toll-Like Receptor 4 Endocytosis and Macrophage Activation. *Immunity* **48**, 59–74.e5 (2018).
25. Baratchi Sara, *et al.*, Transcatheter Aortic Valve Implantation Represents an Anti-Inflammatory Therapy Via Reduction of Shear Stress-Induced, Piezo-1-Mediated Monocyte Activation. *Circulation* **142**, 1092–1105 (2020).
26. R. Goswami, *et al.*, TRPV4 calcium-permeable channel is a novel regulator of oxidized LDL-induced macrophage foam cell formation. *Free Radic. Biol. Med.* **110**, 142–150 (2017).
27. M. Janabi, *et al.*, Oxidized LDL-induced NF-kappa B activation and subsequent expression of proinflammatory genes are defective in monocyte-derived macrophages from CD36-deficient patients. *Arterioscler Thromb Vasc Biol* **20**, 1953–1960 (2000).
28. A. V. Poznyak, *et al.*, Overview of OxLDL and Its Impact on Cardiovascular Health: Focus on Atherosclerosis. *Front Pharmacol* **11**, 613780 (2021).
29. D. Toobian, P. Ghosh, G. D. Katkar, Parsing the Role of PPARs in Macrophage Processes. *Frontiers in Immunology* **12** (2021).

- 1 30. G. Graham, Disparities in Cardiovascular Disease Risk in the United States. *Curr Cardiol Rev* **11**, 238–245 (2015).
2 31. F. Bartoli, *et al.*, Global PIEZO1 Gain-of-Function Mutation Causes Cardiac Hypertrophy and Fibrosis in Mice. *Cells*
3 **11**, 1199 (2022).
4

5 **Figure Legends**

6
7 **Figure 1: Piezo1 depletion suppresses Ca²⁺ activity and oxLDL uptake.** (a-c) Representative
8 GCaMP6f/tdTomato or Green/Red (G/R) ratio images (a) as well as traces of individual Ca²⁺ events (b),
9 and quantification of number of Ca²⁺ events and fraction of cells showing Ca²⁺ elevations (c), taken from
10 a 7-minute time-lapse video of siControl and siPiezo1 treated Salsa6f-expressing BMDMs both with and
11 without oxLDL exposure. Asterisks denote the occurrence of a Ca²⁺ event. Data obtained from N= 7-8
12 videos, letters on top of graphs indicate statistical significance of $p < 0.05$ among groups as determined
13 by Student's t-test. (d) Representative images (top) and mean fluorescence intensity quantification
14 (bottom) of oxLDL uptake. (e) Representative Western blots (top) and quantification (bottom) of CD36
15 and SRA1 in BMDMs isolated from *CTRL* and *Piezo1^{ALysM}* mice following oxLDL treatment. (f)
16 Representative images (top) and total fluorescence intensity quantification of oxLDL uptake (bottom) in
17 *CTRL* and *Piezo1^{ALysM}* BMDMs cultured on 1kPa and 280kPa polyacrylamide hydrogels. Error bars denote
18 mean \pm SD for a minimum of three independent experiments, * $p < 0.05$ as determined by Student's t-test.
19

20 **Figure 2: Piezo1 GOF enhances oxLDL uptake.** (a) Representative images (top) and mean fluorescence
21 intensity quantification of oxLDL uptake (bottom) in BMDMs isolated from *CTRL* and *Piezo1^{GOF}* mice.
22 (b) Representative Western blots (top) and quantification (bottom) of CD36 and SRA1 in BMDMs
23 isolated from *CTRL* and *Piezo1^{GOF}* mice following oxLDL treatment. (c) Representative images (top) and
24 mean fluorescence intensity quantification of oxLDL uptake over time (bottom) in BMDMs isolated from
25 *CTRL* and *Piezo1^{GOF}* mice. Error bars denote mean \pm SD for a minimum of three independent experiments,
26 * $p < 0.05$ as determined by Student's t-test.
27

28 **Figure 3: Piezo1 enhances atherosclerotic plaque formation *in vivo*.** (a) Representative RNAscope
29 images of *Piezo1* in a cross section of the aortic arch in control AAV-Luc and AAV-PCSK9 treated mice
30 following a three-month high fat diet. (b) Representative en-face images of aortas isolated from control
31 and *Piezo1^{ALysM}* mice stained with Oil Red O (ORO) (left) and analysis of percent plaque area across
32 surface of the aorta (right). Darker data points denote male mice while lighter data points denote female
33 mice. Error bars denote mean \pm SD for twelve independent experiments, * $p < 0.05$ as determined by
34 Student's t-test. (c) A representative image of histology sections from isolated aortas stained with ORO
35 (left) and analysis of percent vessel lumen occlusion. Error bars denote mean \pm SD for five independent
36 experiments, * $p < 0.05$ as determined by Student's t-test.
37

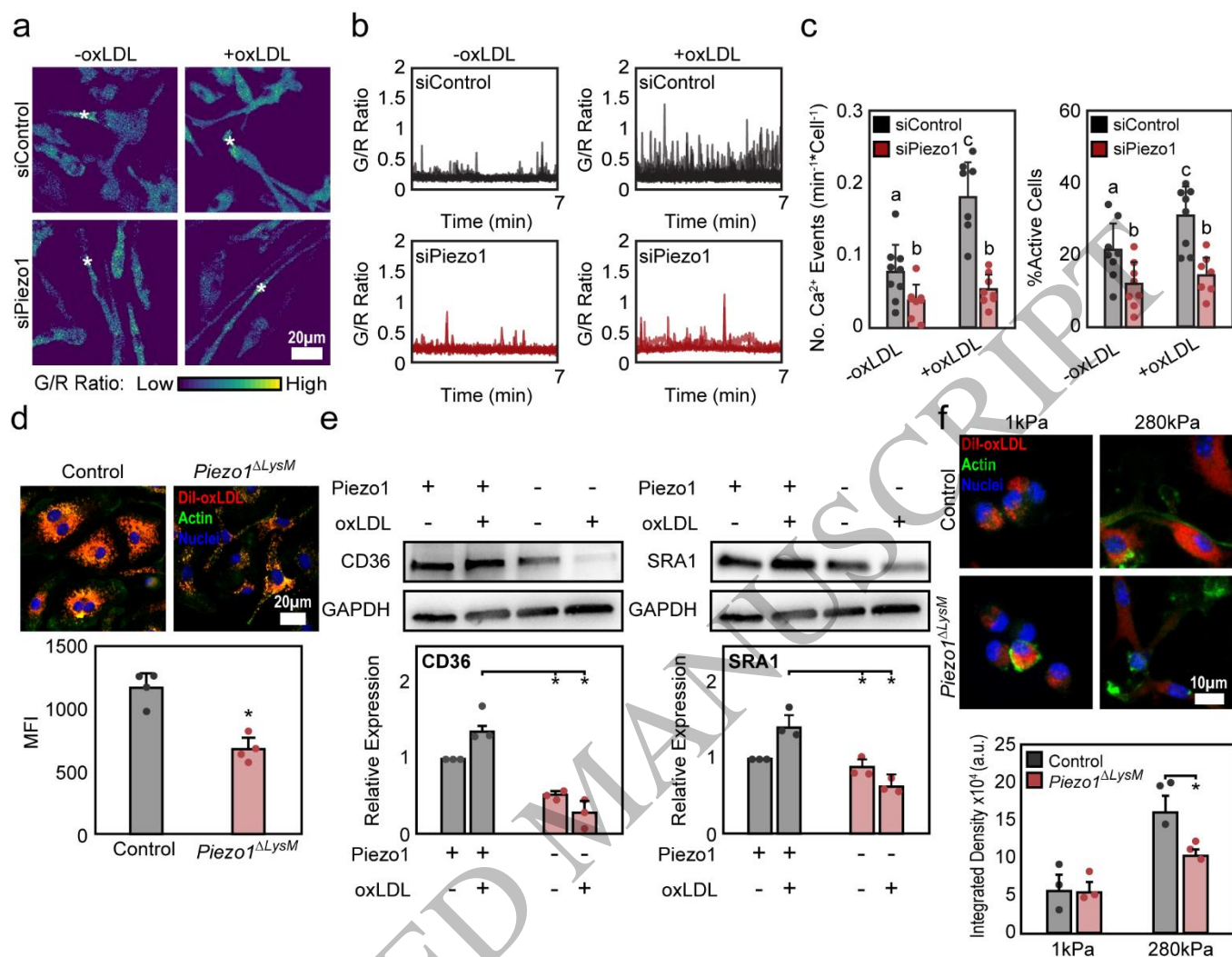


Figure 1
178x139 mm (x DPI)

1
2
3
4

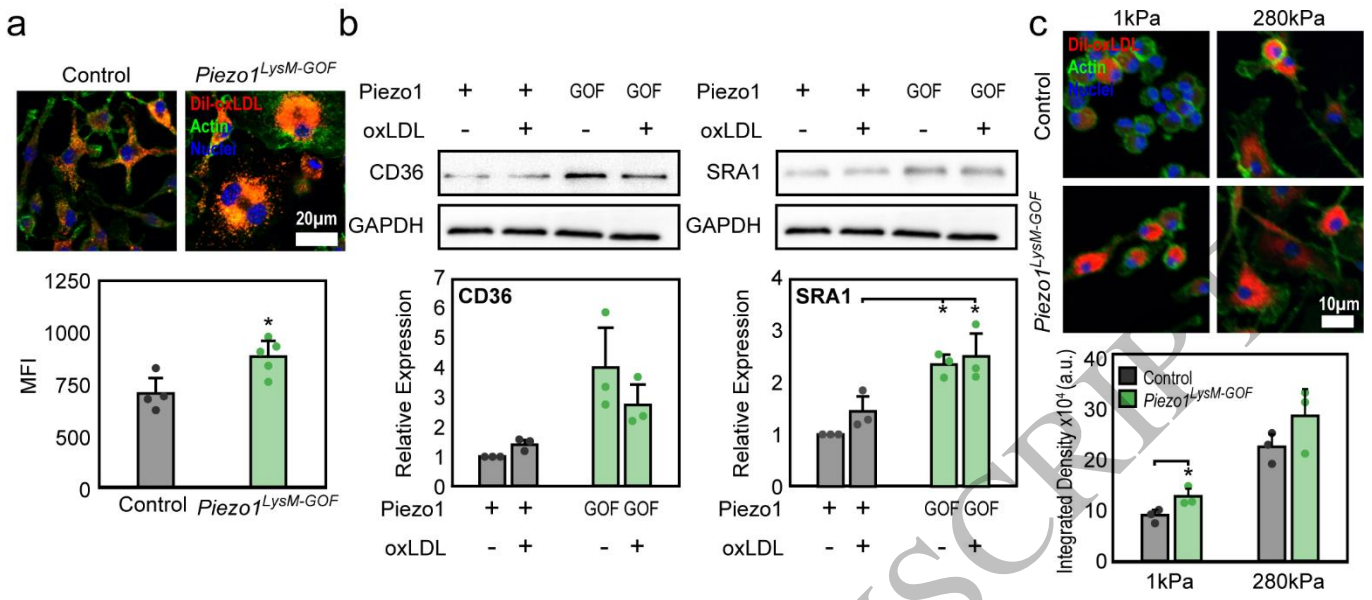


Figure 2
180x78 mm (x DPI)

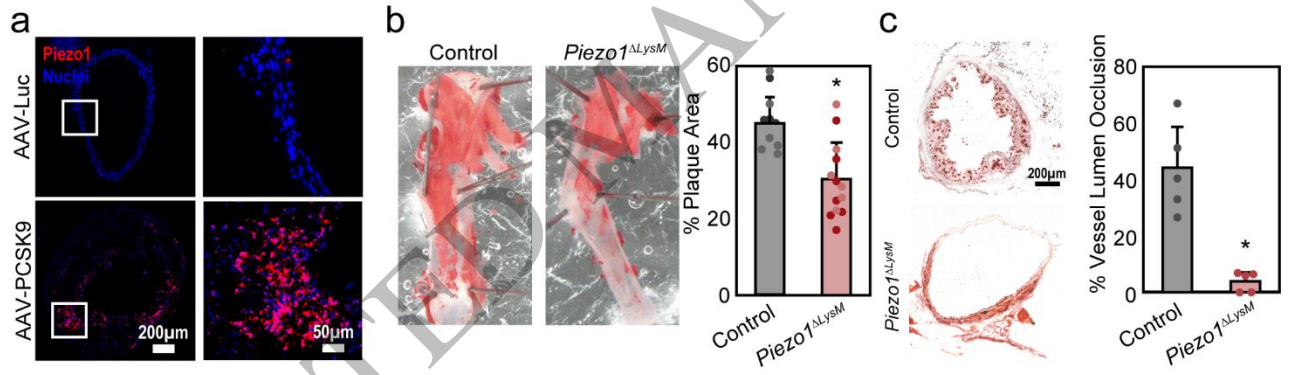


Figure 3
168x49 mm (x DPI)

1
2
3
4

5
6
7